Ultrasonics 98 (2019) 7–14

Contents lists available at ScienceDirect

Ultrasonics

journal homepage: www.elsevier.com/locate/ultras

The effects of thermo-mechanical load on the vibrational characteristics of ultrasonic vibration system

Bo Zhao[a], Wenbo Bie[a,*], Xiaobo Wang[a], Fan Chen[b], Yi Wang[a], Baoqi Chang[a]

[a] School of Mechanical and Power Engineering, Henan Polytechnic University, Jiaozuo, Henan, China
[b] School of Electrical and Mechanical Engineering, Pingdingshan University, Pingdingshan, Henan, China

ARTICLE INFO

Keywords:
Ultrasonic machining
Vibration system
Vibrational characteristic
Thermo-mechanical load
Dynamic model

ABSTRACT

The vibrational characteristics of ultrasonic vibration system play an important role in the stability and processing effect in ultrasonic machining. In this study, a theoretical analysis and experimental verification were employed to investigate the effect of the thermo-mechanical load on the vibrational characteristics of ultrasonic vibration system. Initially, a dynamic model was designed to analyze the influence of the thermo-mechanical load on the vibration characteristics. Based on the model, the single variable method was adopted to explore the effect of different mechanical loading and the rigidity coefficient of the tool on the vibrational characteristics. Then the experiment was conducted by imposing variable loads on the tool end face, and the amplitude, current, frequency and temperature of ultrasonic system were measured. Finally, the ultrasonic vibration drilling test was conducted to verify the experimental results. It was observed that the ultrasonic amplitude initially increased and later decreased with the increase in static load. In addition, with the increase in static load, the thermal effect was significant and the ultrasonic frequency presented a similar tendency, as the ultrasonic amplitude. Meanwhile, the variation of ultrasonic frequency was not significant under the thermo-mechanical load. The results of this study could provide a favorable reference in the design of an ultrasonic vibration system and selection the different tools in ultrasonic machining.

1. Introduction

Ultrasonic machining is a non-traditional mechanical processing method and widely utilized for the machining both conductive and non-metallic materials [1]. During the processing, the vibrational tool leads the abrasive particles contained in the slurry to impact the workpiece surface, thereby causing the removal of the material by micro-chipping, mechanical abrasion, cavitation effects and chemical action [2]. Simultaneously, it reduces the cutting force [3], cutting temperature [4], and improves the integrity of the workpiece surface [5,6]. The ultrasonic machining is a compound machining process, in which some of its processing variables are related to the feed rate of the tool and others are related to ultrasonic parameters, such as the vibration amplitude and the vibration frequency. The machining effect is generally determined by the design of an ultrasonic vibration system. However, when there is an imposed load on the vibration system, the characteristic parameters such as the ultrasonic amplitude and resonant frequency changes at some extent [7].

In general, during the ultrasonic machining, the whole vibration system is expected to run at an optimized performance, wherein the ultrasonic amplitude should reach a peak value at the resonant frequency. Since it is difficult to measure the ultrasonic amplitude during the processing, the ultrasonic vibration is supposed to be stable or unchangeable in the ultrasonic machining, without considering the influence of various processing parameters. Cong et al. using the theoretical and experimental results indicated that the cutting fore in the rotary ultrasonic machining (RUM) decreased with an increase in the ultrasonic amplitude [8]. In other words, the RUM was sensitive to the load generated during the material removal process and the cutting force exhibited a significant effect on the actual ultrasonic amplitude. It was concluded by Wang et al. [9] that the feed rate demonstrated a significant influence on the cutting force in the RUM process, and the augment of the cutting force in RUM led to a decrease in the actual ultrasonic amplitude, when the frequency was tuned at the resonant frequency. Thus, the ultrasonic vibration was significantly influenced by the processing parameters during its operation. Moreover, the ultrasonic vibration amplitude has exhibited a direct effect on the output variables in RUM [10–13]. It is significant to elucidate the experimentally observed phenomena by measuring the ultrasonic amplitude in RUM. Till date, four methods have been reported for the

* Corresponding author.
E-mail address: wenbo187120@163.com (W. Bie).

https://doi.org/10.1016/j.ultras.2019.05.005
Received 30 November 2018; Received in revised form 1 April 2019; Accepted 20 May 2019
Available online 21 May 2019

measurement of the ultrasonic amplitude; including two direct measuring methods *viz.* the optical vibration sensor method and the dial indicator method, and the other two indirect measuring methods *viz.* the microscopic observation method and the observation cutting force variation [11,14,15]. The former two methods could not be directly utilized to measure the ultrasonic amplitude during the RUM processing. The microscopic observation method was only used for the measurement of ductile materials under RUM. The ultrasonic amplitude in brittle materials was obtained through a mechanistic calculation model between the ultrasonic vibration amplitude and the cutting force in RUM of brittle materials. However, the method of ultrasonic amplitude measurement did not consider the thermal effects in RUM, and only analyzed the effect of the ultrasonic amplitude on the processing. It is well known that the ultrasonic amplitude significantly depends on the resonant frequency in ultrasonic machining. In other words, the deviation between the turning frequency and the resonant frequency significantly affects the characteristics of ultrasonic vibration. Considering the state of the art regarding publications, few literatures were used to report the vibrational characteristics under the action of thermal-mechanical load. Wang et al. [16] considered the effect of the thermal load on the vibration system, and explored the stability of the vibration system under the thermo-mechanical load during RUM. It was concluded that the resonant frequency increased with the increase in the mechanical. In contrast, it decreased with the increase in thermal load. In their experimentation, they adopted the change in the ultrasonic power to observe the vibrational characteristics in the processing. Nevertheless, the relationships between the thermal-mechanical load and the vibrational characteristics were not directly obtained in the experiment.

Consequently, it is of great significance to explore the effect thermo-mechanical load on the vibrational characteristics on the ultrasonic vibration system. In this study, the vibrational characteristics of the ultrasonic system under thermo-mechanical load were investigated. Initially, the dynamic model of the vibration system was established. Subsequently, the relationship between the thermal-mechanical load and the ultrasonic vibrational characteristics was directly obtained by the experimental measurement, and the current was utilized to monitor the stability of the ultrasonic vibration. Finally, the effect of the thermo-mechanical load on the vibration system was verified using the ultrasonic vibration drilling test.

2. Theoretical analysis

2.1. Establishment of the dynamic model

The ultrasonic vibration system was composed of the transducer, front cover, horn and tool. In the ultrasonic machining, the load of the vibration system is usually variation with the tool wear. Meanwhile, the variation of the load brings nonlinearity to the vibration system, affects the vibrational characteristics of the ultrasonic vibration system, and causes instability in the process [17]. The vibration system under the load should follow the nonlinear load variation rule, in which the load should be equivalent to the viscoelastic amplitude limiter, namely the Kelvin model [18]. It is assumed that the shape of horn was cylindrical, and the material of construction of the ultrasonic vibration system was an isotropic homogeneous material. The dynamic model was exerted as shown in Fig. 1. The imposed load was equivalent to a linear spring

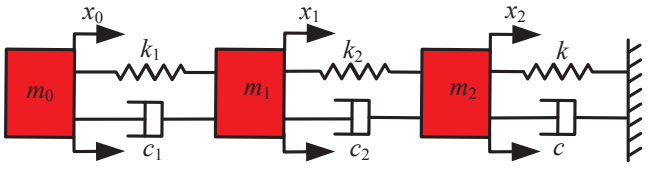

Fig. 1. Simplified model of ultrasonic vibration system.

with rigidity coefficient k and damping coefficient c.

When the load was superimposed on the end face of tool, the dynamic equation of the system can be obtained as follows.

$$\begin{bmatrix} m_1 & 0 \\ 0 & m_2 \end{bmatrix}\begin{bmatrix} \ddot{x}_1 \\ \ddot{x}_2 \end{bmatrix} + \begin{bmatrix} c_1 + c_2 & -c_2 + c_3 \\ -c_2 + c_3 & c_2 - c_3 \end{bmatrix}\begin{bmatrix} \dot{x}_1 \\ \dot{x}_2 \end{bmatrix} + \begin{bmatrix} k_1 + k_2 & -k_2 + k \\ -k_2 & k_2 - k \end{bmatrix}\begin{bmatrix} x_1 \\ x_2 \end{bmatrix} = \begin{bmatrix} (k_1 + jwc_1)X_0 e^{jwt} \\ 0 \end{bmatrix} \quad (1)$$

On the Laplace transformation of Eq. (1), the transfer function under imposed load can be written as follows.

$$G(s) = \frac{c_1c_2s^2 + (k_1c_2 + k_2c_1)s + k_1k_2}{m_1m_2s^4 + [m_2(c_1 + c_2) + m_1(c_2 - c_3)]s^3 + [m_2(k_1 + k_2) + c_1(c_2 - c_3) + (k_2 - k)]s^2 + [k_1(c_2 - c_3) + c_1(k_2 - k)]s + k_1(k_2 - k)} \quad (2)$$

where m_0 is the quality of the piezoelectric ceramic parts, m_1 is the total mass of the preloaded bolt and front cover, m_2 represents the total mass of booster and tool, c is the damping coefficient, c_1 is the damping coefficient of the preloaded bolt and front cover, c_2 is the damping coefficient of booster and tool, k is the spring rigidity coefficient, k_1 is the rigidity coefficient of preloaded bolt and front cover, k_2 is the rigidity coefficient of booster and tool, x_0 is the displacement of the piezoelectric ceramics, x_1 is the displacement of preloaded bolt and front cover, and x_2 is the displacement of booster and tool.

Eq. (2) shows that the variation of the rigidity coefficient k and the damping coefficient c influences the transfer function of the vibration system. It is assumed that the imposed load F on the tool end face complies with the law of sinusoidal variation. In order to gain the relationship between the load and rigidity coefficient k and the damping coefficient c, the dynamic response model of load was introduced as follows.

$$F = k_{3i}x + c\dot{x} = k_{3i}A\sin 2\pi ft + cA2\pi f\cos 2\pi ft = A\sqrt{k_{3i}^2 + (c2\pi f)^2}\sin(2\pi ft + \arccos\frac{k_{3i}}{\sqrt{k_{3i}^2 + (c2\pi f)^2}}) \quad (3)$$

where k_{3i} denotes the rigidity coefficient of tool, and the subscript i represents the tool 1 and 2.

From the knowledge of material science [19], k_3 is directly proportional to the Young's Modulus E of the material with a proportionality coefficient of λ, which was deduced as:

$$k_3 = \lambda E \quad (4)$$

where E is Young's Modulus. It is well known that the Young's Modulus E of a material is related to the temperature T. For tungsten steel, the Young's Modulus E will decrease with an increase in temperature T. Moreover, ΔE can be defined as the change in E due to an increase in the temperature. When the temperature increases, the rigidity coefficient k_3' of the tool can be denoted as follows.

$$k_3' = \lambda(E - \Delta E) \quad (5)$$

Eq. (5) indicates that the rigidity coefficient decreased with an increase in the temperature. Simultaneously, it can be seen from Eq. (3), when rigidity coefficient k and the damping coefficient c were constant, the variation load of the vibration system affected the amplitude and the frequency to a certain extent.

2.2. Determination of the dynamic model parameters

The parameter of tools exhibits a significant influence on the load variation of the vibration system. Since the damping coefficient has a little influence on the temperature change and mechanical load [16], its effect on the vibration characteristics of the vibration system can be neglected. In order to obtain the influence of the different rigidity coefficients on the vibration characteristics, two tools with different outer diameter made of tungsten steel were used in this experiment.

Table 1
Parameters of each segment in ultrasonic vibration system.

Component	Material	Density (kg/m^3)	Elastic modulus (N/m^2)	Parameters
Piezo-ceramics	PZT-4	7700	6×10^{10}	$m_0 = 116.054 \times 10^{-3}\ kg$
Pre-load bolt and Front cover	45steel	7890	21×10^{10}	$m_1 = 193.239 \times 10^{-3}\ kg$, $c_1 = 0.005$ $k_1 = 40.3 \times 10^7\ N/m$
Horn	45steel	7890	21×10^{10}	$m_2 = 420.919 \times 10^{-3}\ kg$, $c_2 = 0.005$ $k_2 = 25.08 \times 10^7\ N/m$
Tool 1	tungsten steel	7290	40×10^{10}	$k_{31} = 30.55 \times 10^7\ N/m$, $c_3 = 0.008$
Tool 2	tungsten steel	7290	40×10^{10}	$k_{32} = 54.31 \times 10^7\ N/m$, $c_3 = 0.008$

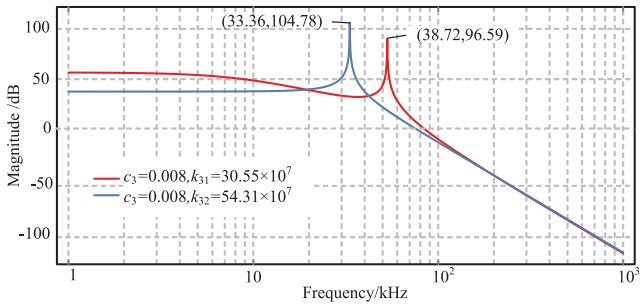

Fig. 2. Bode diagram of the vibration system under different load parameters.

The outer diameter of the first tool (named tool 1) was 6 mm, and the outer diameter of the second tool (named tool 2) was 8 mm. At ambient temperature T_0 of 25 °C, the parameters of each segment in the vibration system are shown in Table 1.

On substituting the above parameters into Eq. (2), the Bode diagram of vibration system under different parameters can be plotted with the Mathematics software. Fig. 2 presents variation in the frequency and amplitude under different rigidity coefficients. Compared with the frequency and amplitude under the rigidity coefficient k_{31}, the frequency decreased by 13.8% and the amplitude increased by 8.4% respectively. Thus, the frequency decreased and the amplitude increased with the increase in rigidity coefficient.

With the increase in temperature, according to Eq. (5), the rigidity coefficient is $k'_{31} = 29.92 \times 10^7\ N/m$ at the temperature T_1 of 96 °C. The influence of the load on the amplitude and frequency at different temperatures was plotted. Fig. 3 presents the effect of the mechanical load on the amplitude under different temperatures. Compared to the amplitude at the temperature T_0, the amplitude at the temperature T_1 decreased by 5.7%. In contrast, as presented in Fig. 4, the frequency at the temperature T_1 decreased by 0.51%.

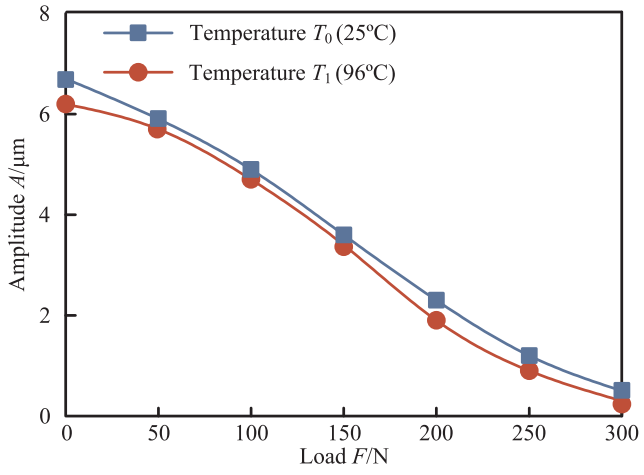

Fig. 3. Effects of the mechanical load on amplitude under different temperatures.

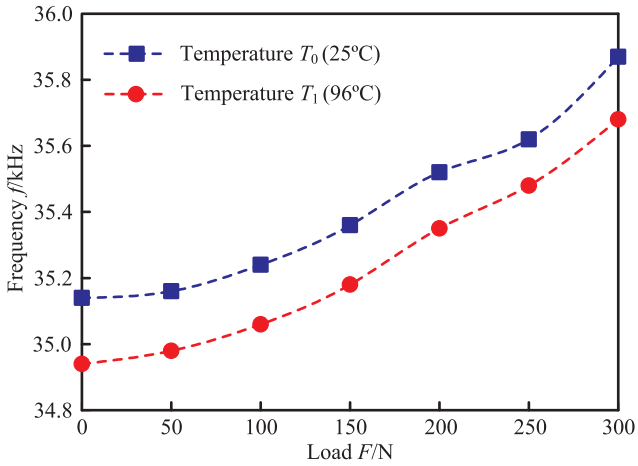

Fig. 4. Effect of mechanical load on frequency under different temperatures.

3. Experiment

3.1. Experimental setup and methodology

The experiment was performed on X8130 universal tool milling machine. The test principle employed is shown in Fig. 5. The measurement device leadingly included the ultrasonic vibration system, the load measurement system and the amplitude measurement system. The ultrasonic vibration system was composed of the ultrasonic generator, transducer, horn and machining tool. The ultrasonic generator was primarily utilized to convert the alternating current into high-frequency electric oscillation for the ultrasonic vibration system. Then the transducer converted the electric oscillation into mechanical vibration at high-frequency. However, the amplitude of mechanical vibration generated by the transducer was generally too low to be used for mechanical machining. Consequently, the horn was added to amplify the ultrasonic vibrational amplitude to an applicable magnitude. The value of the imposed load was measured by a dynamometer (Kistler 9257B). The ultrasonic amplitude was measured by a laser displacement sensor (KEYENCE LK-G10). In order to measure the temperature during the experiment, the different loads were imposed on the end face of tool for at least 10 min. The temperature was measured with an infrared thermometer (BENETECH GM300).

As shown in Fig. 6, the vibration system was fixed on the dynamometer and the machine table was adjusted to make the squeeze head contact with the tool end face. Then the laser displacement sensor was adjusted to produce the laser signal on the tool end face. The switch of ultrasonic generator was turned on, and a load was imposed on the tool end face through adjusting the workbench vertical movement. The value of load was displayed on computer 1, and the value of amplitude was displayed on computer 2. At the same time, the value of frequency and electric current was obtained from the control panel of the

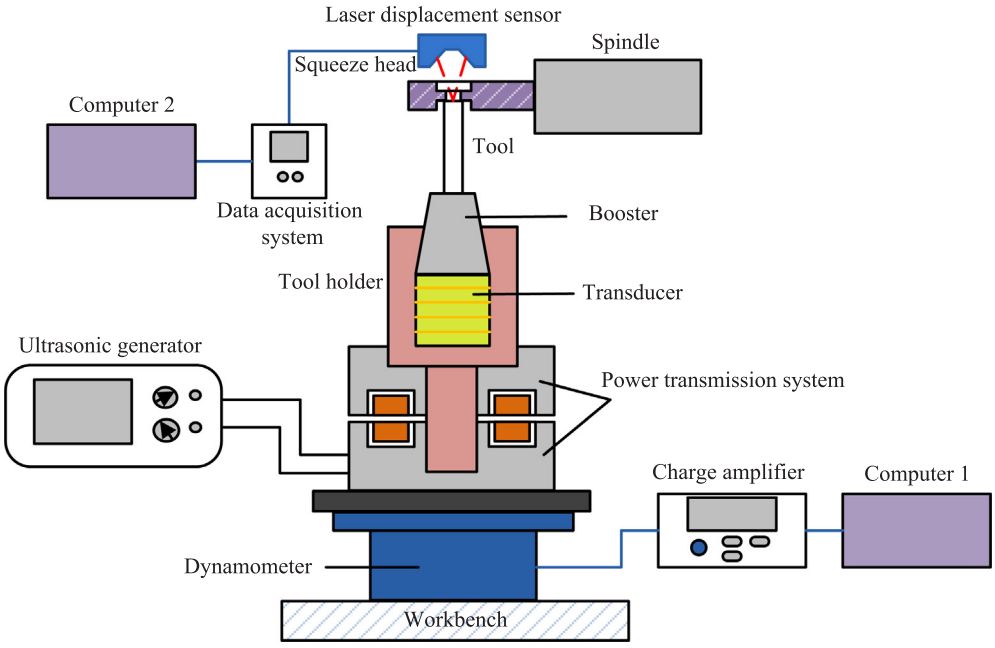

Fig. 5. Schematic of the experiment.

ultrasonic generator.

In order to obtain the relationship between the resonant frequency and the ultrasonic amplitude, the tool 1 and tool 2 were utilized in experiment without any kind of load. Simultaneously, the relationship between the resonant frequency and the electric current was also gained. It was observed from Figs. 7 and 8 that the amplitude and electric current initially increased, while later decreased with the frequency increasing for both tools. The resonant frequency of tool 1 was 35.14 kHz and that of tool 2 was 34.87 kHz, and the corresponding current was 0.21A and 0.23A, respectively.

Experiments were conducted in two groups, in order to obtain the relationship between the ultrasonic amplitude, resonant frequency, temperature, current and the imposed load on the ultrasonic vibration system. The experimental variables are provided in Table 2. Firstly, the ultrasonic frequency was tuned at the resonant frequency of $f_1 = 35.14$ kHz, and a load was imposed on the end face of tool 1. In order to monitor the temperature variation, the time for each load on the tool 1 lasted approximately 10 min. The next experiment was conducted when the temperature of tool was consistent with the ambient temperature. Secondly, the ultrasonic frequency was tuned at resonant frequency of $f_2 = 34.87$ kHz, and a load was imposed on the end face of tool 2. The experiment of tool 2 was performed according to the above-mentioned method. In order to obtain credible data, each test was repeated three times and the measured results were averaged to get the final value.

3.2. Result and discussion

As presented in Fig. 9, the variation tendencies of the ultrasonic amplitude and current for both tools 1 and 2 were identical with the increase in the imposed load. The ultrasonic amplitude initially increased and then decreased with the increase in load, as well as current. Fig. 11 demonstrates the effect of load on the frequency and temperature of the vibration system. When the load was lower than 200 N, the variation of temperature was not significant, and the thermal effect on the vibration system was also negligible. In the stage, the mechanical load primarily acted on the vibration system and led to the resonant frequency increase. Consequently, the amplitude increased with the increased load in the stage. However, the thermal effect was distinct when the load was higher than 200 N, and with the load increasing, the ultrasonic amplitude exhibited a decreasing tendency. Simultaneously, the variation of current for the ultrasonic vibration system presented the same tendency as that of the ultrasonic amplitude. The change of current indirectly reflected the change of amplitude of the vibration system to some extent. Fig. 10 presents the relationship between the current and the ultrasonic amplitude. It could be seen form Fig. 10 that the ultrasonic amplitude increased with the increase in the current. In addition, the current of tool 2 increased by 15.7%, compared with that of the tool 1. Compared with the ultrasonic amplitude of tool 1 under the load 200 N, the amplitude of tool 2 increased by 9.4%. The experimental results were in good consistency with the theoretical analysis.

Fig. 11 presented the relationships between the frequency, temperature and imposed load for both tools 1 and 2. With the increase in the load, the frequency of both tools increased firstly and then decreased, while the temperature of the tool increased until reached thermal equilibrium. When the load was less than 250 N, the frequency increased, however, the frequency decreased when the values of the load were between 250 N and 400 N. The temperature of both the tools 1 and 2 increased when the load was lower than 300 N. When the load was higher than 300 N, the temperature reached a thermal equilibrium and result in the temperature stability. It is well known that the load is always coupled with the thermal effect for ultrasonic vibration system [20]. The effects of thermo-mechanical load on the ultrasonic vibration were presented in Fig. 12. The mechanical load increased the resonant frequency of the ultrasonic machining, while the thermal effect of ultrasonic vibration decreased the resonant frequency. Consequently, the resonant frequency did not monotonously increase with the increasing mechanical load, while due to the effect of thermo-mechanical load, the resonant frequency decreased at the higher temperature.

It can be summarized that, according to the theoretical analysis, the frequency of the vibration system decreased with the increase in the rigidity coefficient, while the amplitude was increased. The experimentally analysis found that the frequency and amplitude of the vibration system tends to increase firstly and then decreased with the increase in load, when the temperature of the system increased.

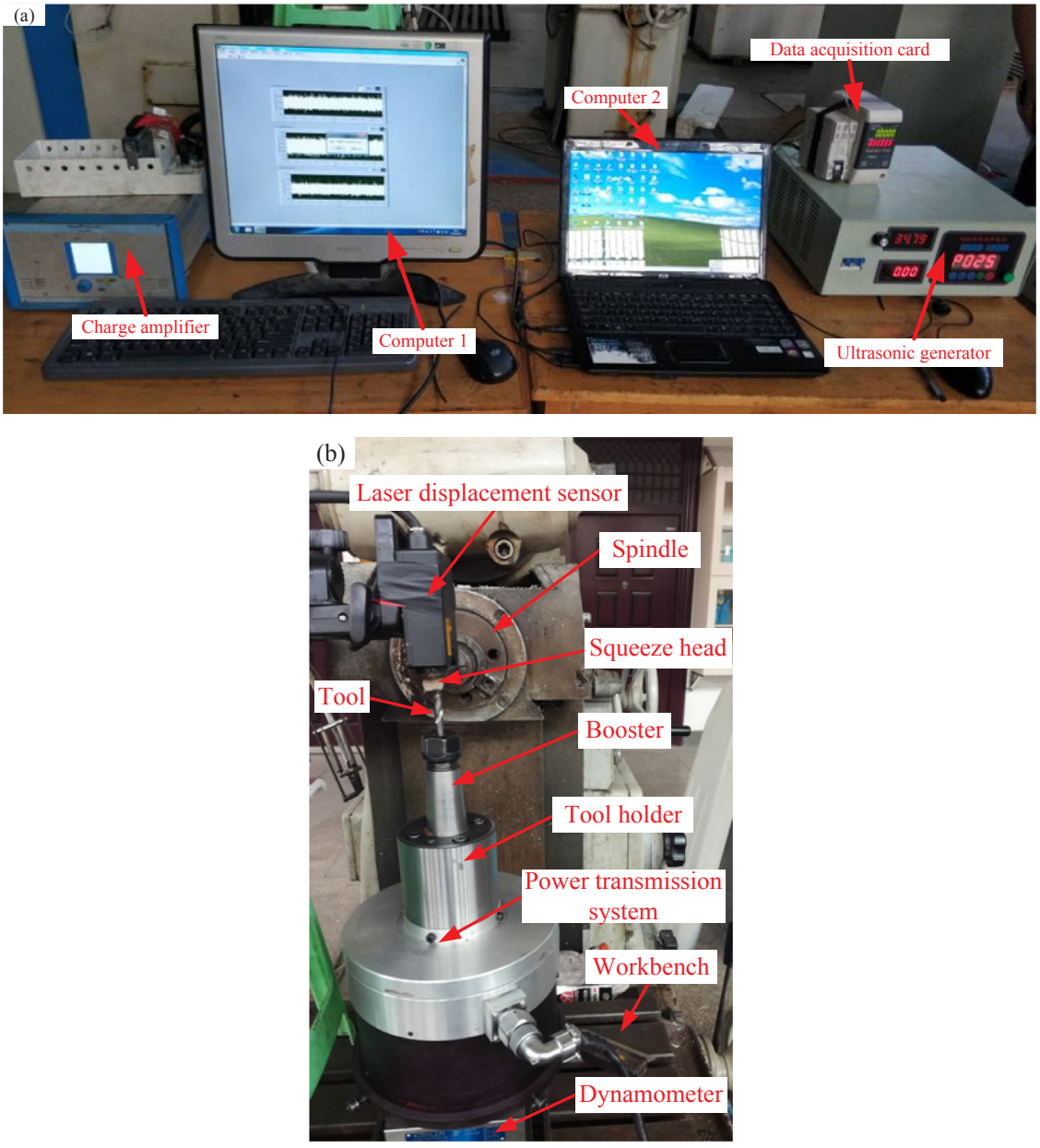

Fig. 6. Experimental apparatus (a) Data acquisition. (b) Experimental installation.

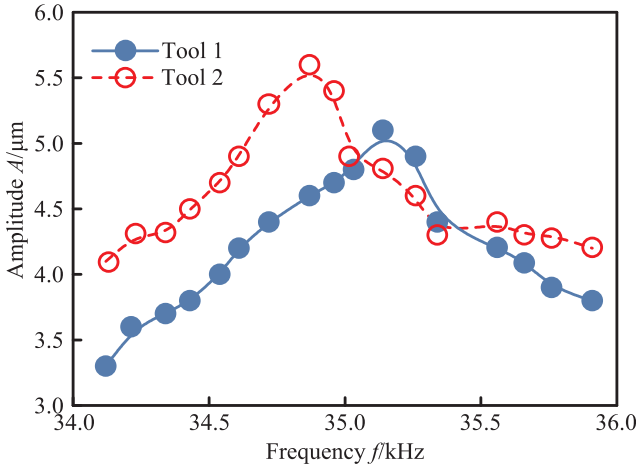

Fig. 7. Relationship between the frequency and amplitude.

4. Ultrasonic vibration drilling test

4.1. Experimental setup and methodology

The ultrasonic vibration drilling test was performed on a modified CNC machine center (VMC850E) assisted with self-designed ultrasonic vibration devices. The experimental setup is shown in Fig. 13. The ultrasonic vibration system was fixed on the spindle of the machining using a clamp. The dynamometer (Kistler9257B) was mounted on the working table of the machine center to hold the workpiece with a jaw vice. The dynamometer was used to record the drilling force along the feed direction during the processing. In order to effectively verify the experimental measurement, both the tools 1 and 2 were used in the ultrasonic vibration drilling test. The test conditions are shown in Table 3. In order to obtain the different loads on the ultrasonic vibration system, the various feed rate were adopted in the test. Under each feed rate, the drilling time lasted for 2 min and the measured process was discrete. The load, temperature, current and ultrasonic frequency

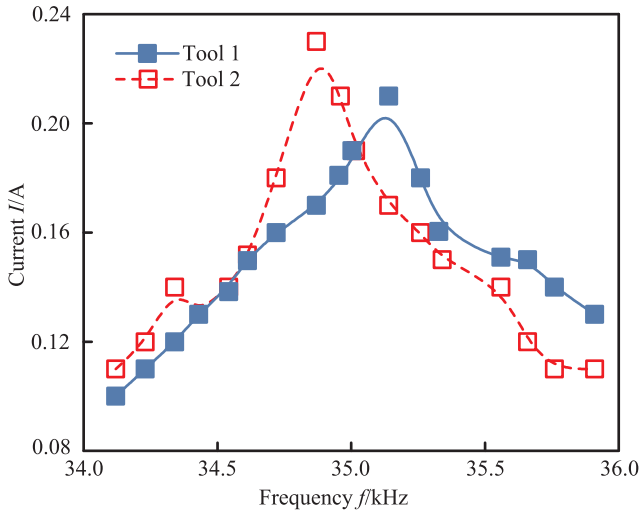

Fig. 8. Relationship between the frequency and current.

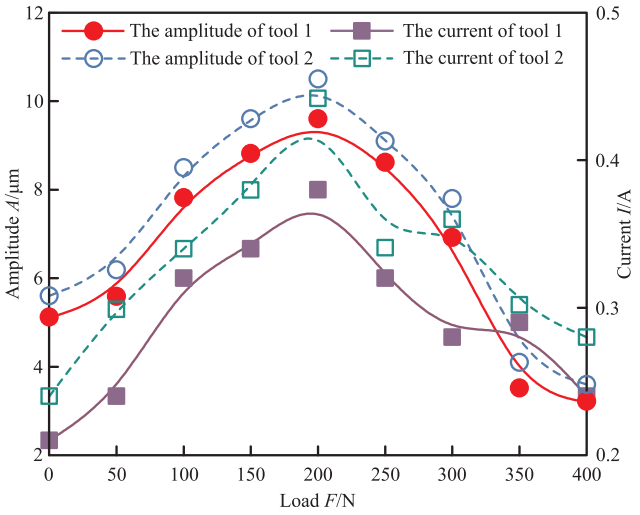

Fig. 9. Influence of load on amplitude and current of the vibration system.

were discretely measured during the drilling time. These measurements were conducted in the next drilling time until the temperature of vibration system was consistent with the ambient temperature. The temperature of vibration system was measured by an infrared thermometer (BENETECH GM300). Simultaneously, the value of frequency and electric current was obtained from the control panel of the ultrasonic generator. In the test, the machine spindle was kept constant at the speed of 1500 r/min. In order to gain reliable data, each test was repeated three times and a final average value was obtained by averaging the measured results.

4.2. Experiment result analysis

In general, the ultrasonic frequency was dramatically higher than the natural frequency of dynamometer (Kistler 9257B), and the measured force was the maximum value of drilling force. Therefore, it was unreasonable to be regarded as an evaluation index of the machining performance. However, the average drilling force could be used as an index to depict the real-time vibration characteristics of the vibration system. As presented in Fig. 14, in the typical curve of the measured drilling force vs time, the average drilling force F_d was calculated by the following equation:

$$F_d = \frac{\int_{t_0}^{t_1} F\mathrm{d}t}{t_1 - t_0} \tag{6}$$

where F was the time-varying measured drilling force, t_0 and t_1 denotes the time when the tool began and completed the drilling, respectively.

As presented in Fig. 15, the average drilling force and the temperature for both the tools of ultrasonic vibration system increased with the increase in the feed rate. Compared with the average drilling force and the temperature of tool 1 under the feed rate 15 mm/min, the force of tool 2 increased by 8.2%, and the temperature increased by 5.5%. The variation of feed rate of both tools was to be equivalent to impose different loads on the vibration system. Since the amplitude of the system cannot be directly measured in the ultrasonic vibration drilling test, as described in Section 3.2, the current change of the system indirectly reflected the change of amplitude of the system to some extent.

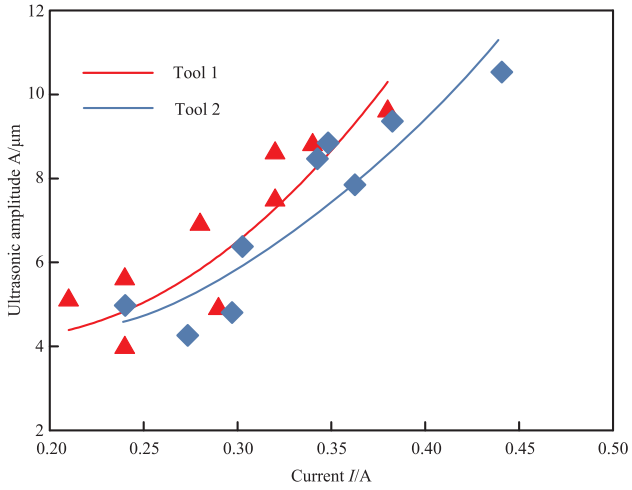

Fig. 10. Relationship between the current and the ultrasonic amplitude.

It can be seen from Fig. 16 that the resonant frequency of the vibration system presented a drift with the feed rate increase, and the current increased firstly and then decreased. When the feed rate was 15 mm/min, the current of tool 2 increased by 17.8% than that of the tool 1. The results indirectly verified that the amplitude increases with the increase of the rigidity coefficient. During the ultrasonic vibration drilling, it was also observed that the feed rate played an important role on the vibrational characteristic. When the feed rate was lower than 15 mm/min, the variation of temperature was not obvious and the thermal effect on the vibration system was also smaller. In the stage, the mechanical load was primarily acting on the vibration system and led to an increase in the resonant frequency and the amplitude with the feed rate increasing. However, the thermal effect was distinct when the feed rate was higher than 15 mm/min, and with the increasing feed rate, the resonant frequency and the ultrasonic amplitude appeared decrease tendency. This result was in good agreement with the experimental results. It also indicated that the mechanical load and the thermal effect

Table 2
Experimental variables.

Experiment	Tool	Frequency (kHz)	Imposed load (N)
Group 1	Tool 1	35.14	0, 50, 100, 150, 200, 250, 300, 350, 400
Group 2	Tool 2	34.87	0, 50, 100, 150, 200, 250, 300, 350, 400

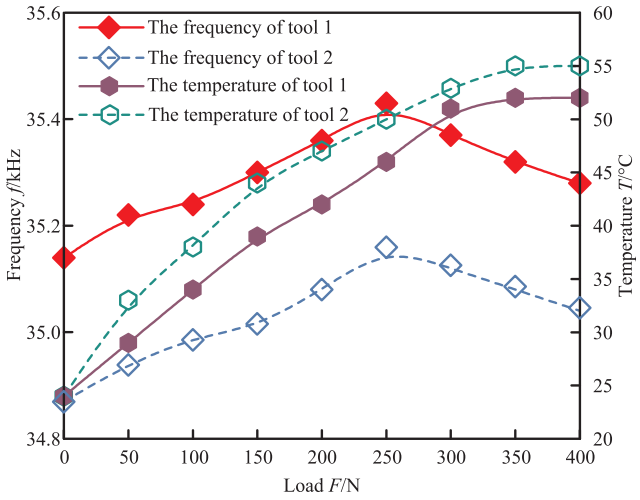

Fig. 11. Influence of load on the frequency and temperature of vibration system.

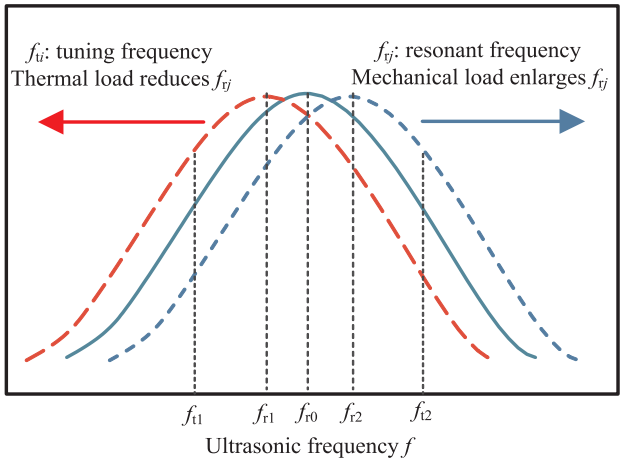

Fig. 12. Relationship between thermal load and mechanical load and resonant frequency.

Table 3
Test conditions during the ultrasonic vibration drilling.

Parameters	Value
Feed rate v (mm/min)	5, 10, 15, 20
Spindle speed (r/min)	1500
Frequency (kHz)	35.14, 34.87
Tool	tool 1, tool 2
Rigidity coefficient of tool (N/m)	30.55×10^7, 54.31×10^7
Damping coefficient of tool	0.008

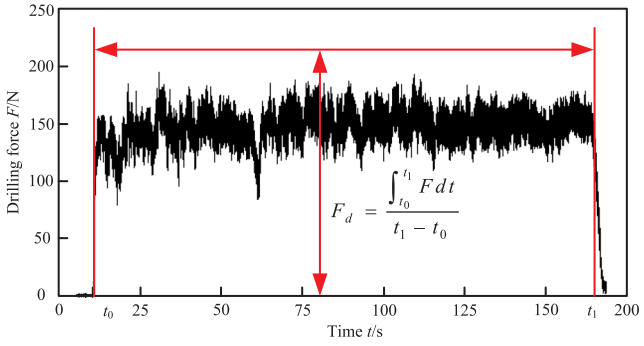

Fig. 14. Calculation of average drilling force.

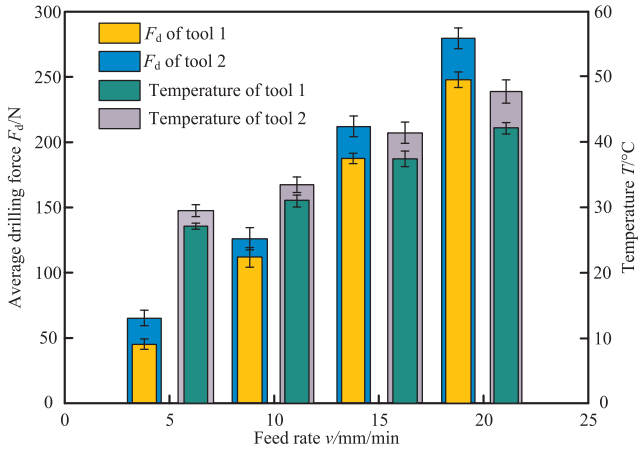

Fig. 15. Influence of the feed rate on average drilling force and temperature.

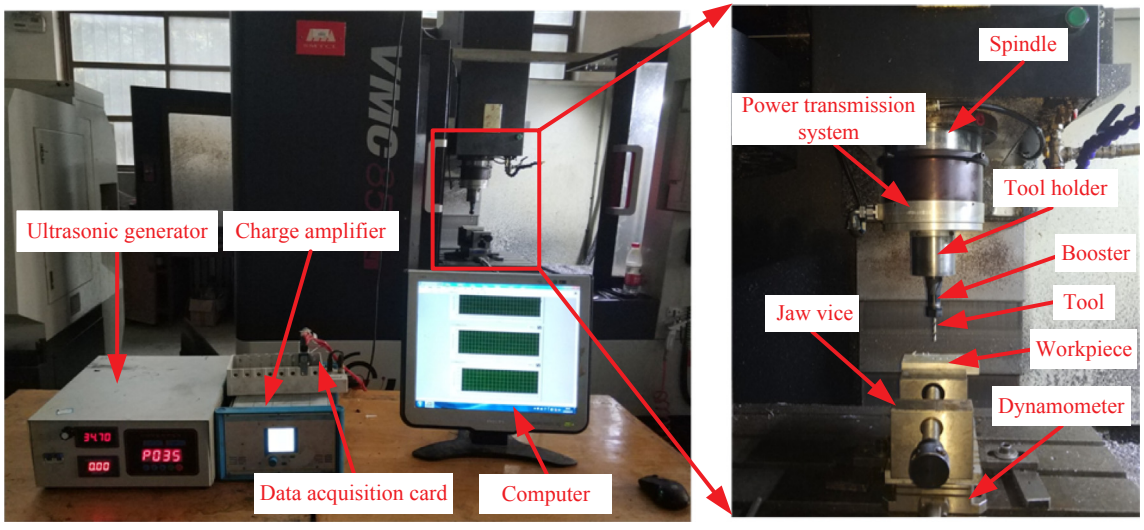

Fig. 13. Setup for the ultrasonic vibration drilling test.

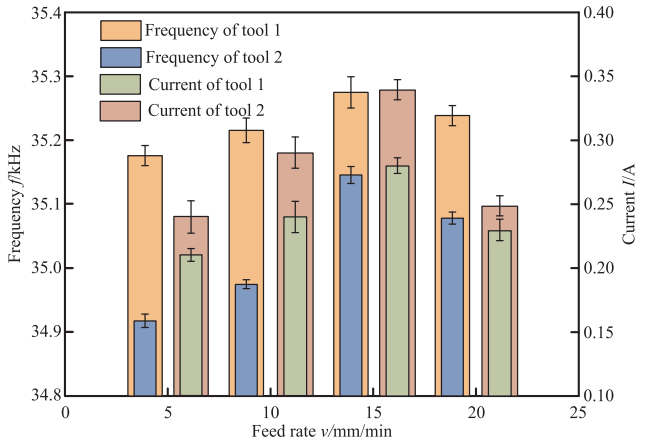

Fig. 16. Influence of the feed rate on current and frequency.

were coupled in the ultrasonic machining, and the action of thermo-mechanical load exhibited a significant effect on the vibrational characteristics.

The action of the thermo-mechanical load on the ultrasonic system in a certain range was responsible for an optimized performance of the whole ultrasonic system. In this study, the rigidity coefficient of the tool and the feed rate dramatically influenced the vibrational characteristics. Therefore, the tool with a higher rigidity coefficient and a reasonable feed rate should be selected during the ultrasonic vibration drilling.

5. Conclusion

The effects of thermo-mechanical load on the vibrational characteristics were investigated in the present study by means of theoretical analysis and a subsequent experimental verification. A theoretical model was developed to reveal the influence of the rigidity coefficient on the frequency and amplitude of the ultrasonic vibration system, and also to demonstrate the effects of thermo-mechanical load. The main conclusions can be obtained as follows:

(1) It was observed that, during the machining of the ultrasonic vibration system, the ultrasonic amplitude and frequency were variable. Under the action of thermo-mechanical load, there was a critical load effect on the vibration system. Before the point of the critical load, the ultrasonic amplitude and the frequency increased with an increase in the static load, while after the critical load, the tendency of ultrasonic amplitude and frequency inversed.
(2) It was experimentally found that the variation in the current of the ultrasonic vibration system presented the same trend as the ultrasonic amplitude. Consequently, to a certain extent, the change of current indirectly reflected the change of amplitude of the vibration system.
(3) In ultrasonic vibration drilling test, the feed rate of the tools was to be equivalent to different load on the vibration system. The variations in the ultrasonic frequency and the current with the increase in feed rate in the test were in good agreement with the measurement experimental results.

Declaration of Competing Interest

The authors declare that no potential conflicts of interest with respect to the research, authorship, and/or publication of this article.

Acknowledgements

The authors gratefully acknowledge the support of the National Natural Science Foundation of China through Grant No. 51475148, U1604255. The authors sincerely acknowledge the Institute of Advanced Manufacturing Technology of Henan Province Key Laboratory, Henan Polytechnic University for their crucial support.

References

[1] J. Kumar, Ultrasonic machining-a comprehensive review, Mach. Sci. Technol. 17 (3) (2013) 325–379.
[2] T.B. Thoe, D.K. Aspinwall, M.L.H. Wise, Review on ultrasonic machining, Int. J. Mach. Tools Manuf. 38 (4) (1998) 239–255.
[3] J. Kumabe, The Foundation and Application of Precision Vibration Cutting, Machinery Industry Press, Beijing, China, 1985.
[4] A. Abdullah, A. Farhadi, A. Pak, Ultrasonic-assisted dry creep-feed up-grinding of super alloy inconel 738LC, Exp. Mech. 52 (7) (2012) 843–853.
[5] J.F.G. Oliveira, E.J. Silva, C. Guo, Industrial challenges in grinding, CIRP Ann.-Manuf. Technol. 58 (2) (2009) 663–680.
[6] H. Chen, W. Zhou, J. Tang, An experimental study of the effects of ultrasonic vibration on grinding surface roughness of C45 carbon steel, Int. J. Adv. Manuf. Technol. 68 (9–12) (2013) 2095–2098.
[7] F.G. Cao, Ultrasonic Machining, Chemical Industry Press, Beijing, China, 2014.
[8] W.L. Cong, Z.J. Pei, X. Sun, C.L. Zhang, Rotary ultrasonic machining of CFRP: a mechanistic predictive model for cutting force, Ultrasonics 54 (2) (2014) 663–675.
[9] J. Wang, P. Feng, J. Zhang, W. Cai, H. Shen, Investigations on the critical feed rate guaranteeing the effectiveness of rotary ultrasonic machining, Ultrasonics 74 (2017) 81–88.
[10] W.L. Cong, Z.J. Pei, T.W. Deines, A. Srivastava, L. Riley, C. Treadwell, Rotary ultrasonic machining of CFRP composites: a study on power consumption, Ultrasonics 52 (8) (2012) 1030–1037.
[11] F.D. Ning, W.L. Cong, Z.J. Pei, C. Treadwell, Rotary ultrasonic machining of CFRP: a comparison with grinding, Ultrasonics 66 (2016) 125–132.
[12] R.P. Singh, S. Singhal, Rotary ultrasonic machining: a review, Mater. Manuf. Process. 31 (14) (2016) 1795–1824.
[13] J. Wang, J. Zhang, P. Feng, P. Guo, Experimental and theoretical investigation on critical cutting force in rotary ultrasonic drilling of brittle materials and composites, Int. J. Mech. Sci. 135 (2018) 555–564.
[14] W.L. Cong, Z.J. Pei, N. Mohanty, E. Van Vleet, C. Treadwell, Ultrasonic vibration amplitude in rotary ultrasonic machining: a novel measurement method and effects of process variables, J. Manuf. Sci. Eng. 133 (3) (2011) 1–6.
[15] F. Ning, H. Wang, W. Cong, A mechanistic ultrasonic vibration amplitude model during rotary ultrasonic machining of CFRP composites, Ultrasonics 76 (2017) 44–51.
[16] J. Wang, P. Feng, J. Zhang, Experimental investigation on the effects of thermo-mechanical load on the vibrational stability during rotary ultrasonic machining, Mach. Sci. Technol. 21 (2) (2016) 239–256.
[17] V.K. Astashev, V.I. Babitsky, Ultrasonic cutting as a nonlinear (vibro-impact) process, Ultrasonics 36 (1998) 89–96.
[18] Y.Q. Yuan, Principle and Application of Modern Ultrasonic, Nanjing University Press, Nanjing, China, 1996.
[19] A.P. Boresi, R.J. Schmidt, O.M. Sidebottom, Advanced Mechanics of Materials, Wiley, New York, 1993.
[20] J. Wang, P. Feng, J. Zhang, Experimental study on vibration stability in rotary ultrasonic machining of ceramic matrix composites: cutting force variation at hole entrance, Ceram. Int. 44 (12) (2018) 14386–14392.